Comparison of CFD Natural Convection and Conduction-only Models for Heat Transfer in the Yucca Mountain Project Drifts

Teklu Hadgu, Stephen W. Webb, and Michael T. Itamura

Sandia National Laboratories, Albuquerque, New Mexico 87185

ABSTRACT

Yucca Mountain, Nevada has been designated as the nation's high-level radioactive waste repository and the U.S. Department of Energy has been approved to apply to the U.S. Nuclear Regulatory Commission for a license to construct a repository. Heat transfer in the Yucca Mountain Project (YMP) drift enclosures is an important aspect of repository waste emplacement. Canisters containing radioactive waste are to be emplaced in tunnels drilled 500 m below the ground surface. After repository closure, decaying heat is transferred from waste packages to the host rock by a combination of thermal radiation, natural convection and conduction heat transfer mechanisms. Current YMP mountain-scale and drift-scale numerical models often use a simplified porous medium code to model fluid and heat flow in the drift openings. To account for natural convection heat transfer, the thermal conductivity of the air was increased in the porous medium model. The equivalent thermal conductivity, defined as the ratio of total heat flow to conductive heat flow, used in the porous media models was based on horizontal concentric cylinders. Such modeling does not effectively capture turbulent natural convection in the open spaces as discussed by Webb et al. (2003) yet the approach is still widely used on the YMP project.

In order to mechanistically model natural convection conditions in YMP drifts, the computational fluid dynamics (CFD) code FLUENT (Fluent, Incorporated, 2001) has been used to model natural convection heat transfer in the YMP emplacement drifts. A two-dimensional (2D) model representative of YMP geometry (e.g., includes waste package, drip shield, invert and drift wall) has been developed and numerical simulations made (Francis et al., 2003). Using CFD simulation results for both natural convection and conduction-only heat transfer in a single phase, single component fluid, equivalent thermal conductivities have been calculated for different Rayleigh numbers. Correlation equations for equivalent thermal conductivity as a function of Rayleigh number were developed for the Yucca Mountain geometry and comparisons were made to experimental data and correlations found in the literature on natural convection in horizontal concentric cylinders, a geometry similar to YMP.

The objective of this work is to compare the results of CFD natural convection simulations and conduction-only calculations that used the equivalent thermal conductivity to represent heat transfer by turbulent natural convection. The FLUENT code was used for both simulations with heat generation boundary condition at the waste package and constant temperature boundary condition 5 meters into the host rock formation. Comparisons are made of temperature contours in the drift air and temperature profiles at surfaces of the different engineered components using the two approaches. The results show that for the two-dimensional YMP geometry considered,

the average surface temperatures of the CFD natural convection and conduction-only using the equivalent thermal conductivity are similar and the maximum local temperature differences for the different surfaces were within two 2°C. The differences in temperature profiles reflect the use of a constant equivalent thermal conductivity. The effect of the differences is discussed.

1. INTRODUCTION

In order to assess the performance of the repository, studies of heat transfer and fluid flow processes in the emplacement drifts are required. Thermal radiation and turbulent natural convection in the YMP enclosures are important part of the heat transfer and fluid flow mechanisms of the post-closure in-drift environment. To better understand these mechanisms, CFD models have been developed and the models have been used to provide simplified correlations. These simplified correlations are for total heat transfer and can be used in an equivalent thermal conductivity approach in a porous media code. This paper describes some of these models and correlations, and assesses the performance of the correlations.

This work summarizes two-dimensional heat transfer and fluid flow simulations in the YMP drift using the CFD software FLUENT. The work described in this report is a continuation of the CFD simulations for YMP application described in Francis et al. (2003). Heat generated by the decay of radioactive materials in spent nuclear fuel rods will be transmitted to the rock formation through materials in the drift and open spaces. In this study comparison is made of CFD natural convection and conduction-only simulation results. The model geometry consists of an emplacement drift, waste package, titanium drip shield, and a crushed rock invert providing a flow barrier at the bottom of the drift. Figure 1 shows a schematic diagram of the geometry modeled. The drift diameter is 5.5 meters. The waste packages are between 1.5 and 2.1 meters in diameter.

In the CFD models presented in this paper, the heat generated by the waste packages is transmitted through radiation, natural convection and conduction. Natural convection occurs in the open spaces between the waste package and the drip shield, and between the drip shield and the drift wall. The primary focus of this study is use of heat generation boundary conditions in the waste package and constant temperature boundary conditions five meters into the rock formation. The two-dimensional CFD simulations of heat transfer in the YMP geometry are then compared to conduction-only simulations that use equivalent thermal conductivity correlations. These correlations are a function of dimensionless numbers and are expected to be applicable to variable wall temperature situations. The models did not include evaporation or condensation processes in the emplacement drift. Because of the two-dimensional modeling approach, axial heat transfer mechanisms have not also been considered.

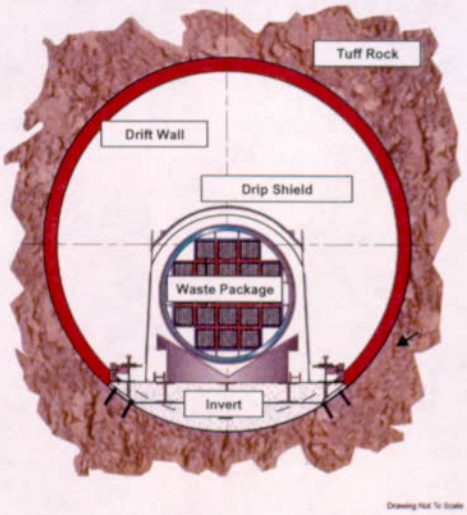

Figure 1. Cross-section of the modeled drift. The drift wall, invert, drip shield, host rock, and waste packages were all modeled.

1.1 Background

Natural convection heat transfer in horizontal concentric (or eccentric) cylinders with a hotter inner cylinder and a cooler outer wall has been the subject of concerted study over the past three decades. The geometry is similar to, but not identical to, the YMP geometry shown in Figure 1. Francis et al. (2003) give an extensive overview of the literature on the subject. Numerous experimental, correlation, and modeling studies have been presented in the literature. Most of these studies were based on very small inner and outer cylinder radii (on the order of a few centimeters) and gap-widths (1.9 cm $\leq L \leq$ 7.1 cm). Kuehn and Goldstien (1976a, 1976b, 1978) provided experimental and theoretical analysis of natural convection heat transfer in concentric cylinders with diameter ratio (Di/Do) of 2.6. Their work is widely accepted and has been used in various studies. For YMP applications interest is focused on large gap widths (on the order of 0.5 m or greater) and larger radius ratios ($R_o/R_i \approx$ 3.2-3.5) than used in most of the experimental studies.

Most of the concentric cylinder modeling studies consider gases (Pr $\approx$ 0.7) as the working fluid in the annulus (e.g., Kuehn and Goldstein (1976), (1978). In the present study air is used as the working fluid which has a Prandtl number of approximately 0.7.

The transition gap-width Rayleigh number for turbulence is about 10^6 (e.g. Kuehn and Goldstein (1978). For Rayleigh numbers greater than the transition value, the annulus internal flow conditions are characterized by a turbulent upward moving plume above the inner cylinder and a turbulent downward flow against the outer wall. Stagnation regions exist near the top where the plume impinges on the outer cylinder and over the entire bottom of the annulus. A low velocity laminar region exists in the annulus away from the walls. Turbulent flow conditions in the annulus are typically obtained either through the length scale (e.g., gap width) or the operating

conditions (e.g., temperature difference and operating pressure) of the configuration. For the very small gap widths (~ 3 cm) considered in the experiments presented in the literature, air at atmospheric pressure temperatures would not result in turbulent flow (e.g., $Ra_L < 10^6$). Pressurized gases such as nitrogen were often used in experiments to obtain the fluid properties necessary to achieve turbulent Rayleigh numbers for very small gap widths and small temperature differences (Kuehn and Goldstein, 1978).

Most of the experimental data discussed above and presented in the literature are restricted to heat transfer results such as temperature and equivalent thermal conductivity. Experimental measurements of fluid velocity and turbulence quantities for the horizontal annulus configuration have not been published in the literature.

1.2 Equivalent Thermal Conductivity

Modeling of heat transfer and fluid flow in the open areas of the drift using porous medium codes alone by assuming porous medium flow does not allow modeling of natural convection. To solve the problem the drift was modeled as a conduction-only zone with an effective thermal conductivity (Francis et al., 2003). The effective thermal conductivity attempts to model natural convection heat transfer by specifying an enhanced thermal conductivity for use in a conduction-only model. The effective thermal conductivity is defined as (Francis et al, 2003):

$$k_{eff,} = k_{eq} * k_a(\overline{T}) \qquad (1)$$

where k_{eff} = effective thermal conductivity
k_a = thermal conductivity of air which is a function of temperature
k_{eq} = equivalent thermal conductivity

The equivalent thermal conductivity is defined as:

$$k_{eq} = \frac{Q}{Q_{cond}} \qquad (2)$$

where Q = heat transfer rate due to convection and conduction
Q_{cond} = heat transfer rate for conduction-only flow

The equivalent thermal conductivity (k_{eq}) is a dimensionless quantity. The effective thermal conductivity, $k_{eff,}$ includes the effects of natural convection and has units of W/m-K. The stagnant air thermal conductivity (k_a) is a function of the average fluid temperaturewith units W/m-k.
Various authors have attempted to correlate the equivalent thermal conductivity with flow parameters. Kuehn and Goldstein (1976, 1978) provided correlating equations for the equivalent thermal conductivity as a function of Rayleigh (Nusselt) number. As detailed in Section 2 of this paper Francis et al. (2003) generated the equivalent thermal conductivity for two-dimensional natural convection in the YMP drifts using FLUENT runs with and without convection.

2. EQUIVALENT THERMAL CONDUCTIVITY DETERMINATION FOR YMP GEOMETRIES

2.1 Equivalent Thermal Conductivity Obtained Using CFD Simulations

Two-dimensional CFD models with isothermal surfaces were employed to develop heat transfer correlation equations that supply effective thermal conductivities for YMP geometries required by porous media flow models (Francis et al., 2003). The CFD models included heat transfer by conduction and turbulent natural convection only. Thermal radiation was not included because the intent of this heat transfer analysis is to compute an effective thermal conductivity that approximates heat transfer by natural convection only. The CFD models used to create YMP-specific heat transfer correlation equations included different waste package diameters and all of the in-drift components discussed above with the exception of the waste package pedestal (Figure1). Two equivalent thermal conductivity correlations were developed: one for flow conditions inside the drip shield (i.e. the inner annulus between the waste package, the drip shield and the inner invert) and a second for outside the drip shield (i.e. the outer annulus between the drip shield, drift wall and outer invert).

The equivalent thermal conductivity was obtained by running FLUENT with and without gravity. With gravity, natural convection occurs in the annulus. Without gravity, heat transfer is by conduction only. For each geometry and selected temperature difference (between inner and outer surfaces), the CFD model was run in conduction-only mode to get the baseline conduction heat transfer. The total heat flux for a natural convection model was then determined in a CFD simulation. The equivalent thermal conductivity was obtained using Equation 2.

2.1.1 Equivalent Thermal Conductivity inside the Drip Shield

For the region inside the drip shield FLUENT was run with different model parameters (e.g. waste package diameter, temperature difference). The equivalent thermal conductivity values were then plotted as a function of gap-width Rayleigh number. The Rayleigh number for natural convection in an annular space, based on a characteristic gap-width is,

$$Ra_{L_c} = \frac{g\beta\Delta T L_c^{\,3}}{\nu\alpha} \tag{3}$$

where the characteristic gap-width (L_c,) is half the hydraulic and is given by the following relationship:

$$L_c = \frac{2A_c}{P} \tag{4}$$

where A_c is the cross-sectional area and P is the wetted perimeter. It is noted that the characteristic gap-width reduces to the standard gap-width definition, $R_o - R_i$, for a concentric cylinder annulus.

A linear fit on a log-log plot of the equivalent thermal conductivity versus Rayleigh number was used to generate a YMP-specific correlation equation for natural convection heat transfer inside the drip shield. The correlation equation is a function of the Rayleigh number, which is a function of the average temperature, temperature difference across the enclosure, and characteristic gap width. The correlation equation in terms of Rayleigh number is that given by Equation 5 (see Table 1). A more useful form of the correlation equation for the region inside the drip shield is that given by Equation 6 (Table 1).

Note that Equations 5 and 6 are only applicable inside the drip shield. Constraints for temperature difference and characteristic gap width for the YMP-specific correlation equation for natural convection heat transfer are given in Table 1. Thermal properties are evaluated at an average fluid temperature (Note: when using the second form of the equation, $\overline{T}$ is the average fluid temperature in absolute temperature, K). Equations 5 and 6 should be applied within the above constraints when evaluating the equivalent thermal conductivity for YMP geometries inside the drip shield (eccentric placement with invert and drip shield).

2.1.2 Equivalent Thermal Conductivity outside the Drip Shield

A similar correlation equation was obtained for the equivalent thermal conductivity outside the drip shield. For the region outside the drip shield the alternate form of the correlation equation is given by Equation 8 (Table 1).

Note that Equations 7 and 8 are only applicable outside the drip shield. Constraints for temperature difference and characteristic gap width for the YMP-specific correlation equation for natural convection heat transfer are given in Table 1. Thermal properties are evaluated at an average fluid temperature (Note: when using the second form of the equation, $\overline{T}$ is the average fluid temperature in absolute temperature, K).

Equation 8 should be applied within the above constraints when evaluating the equivalent thermal conductivity for YMP geometries outside the drip shield (eccentric placement with invert and drip shield).

Table 1 summarizes each of the natural convection heat transfer correlation equations developed for YMP geometries. Figure 2 illustrates the Kuehn and Goldstein correlation equations (1976 and 1978) for natural convection heat transfer together with Equations 5 and 6. The curve labeled "Kuehn & Goldstein 1978- YMP" was obtained using the Kuehn and Goldstein (1978) correlation equations extended for concentric cylinders using YMP-type geometry representing the waste package and drift wall.

Table 1. Summary of YMP Correlation Equations for Natural Convection Heat Transfer in Enclosures based on CFD simulation results[1]

Location	Correlation Equation	Comments	Eq.
Inside Drip Shield	$k_{eq} = 0.142 Ra_{Lc}^{0.258}$	$4.55x10^4 \le Ra_{L_c} \le 3.53x10^8$	5
	$k_{eq} = 16465 \overline{T}^{1.214} \Delta T^{0.258} L_c^{0.774}$	0.0108 K $\le \Delta T \le$ 27 °C, 0.3m $\le L_c \le$ 0.7m, $\overline{T}$ is the average fluid temperature in K	6
Outside Drip Shield	$k_{eq} = 0.100 Ra_{Lc}^{0.263}$	$1.32x10^6 \le Ra_{L_c} \le 4.05x10^9$	7
	$k_{eq} = 13893 \overline{T}^{1.233} \Delta T^{0.263} L_c^{0.786}$	0.0092 K $\le \Delta T \le$ 23 °C, L_c =1.5m, $\overline{T}$ is the average fluid temperature in K	8

1 - $k_{eff} = k_{eq} * k_o(\overline{T})$

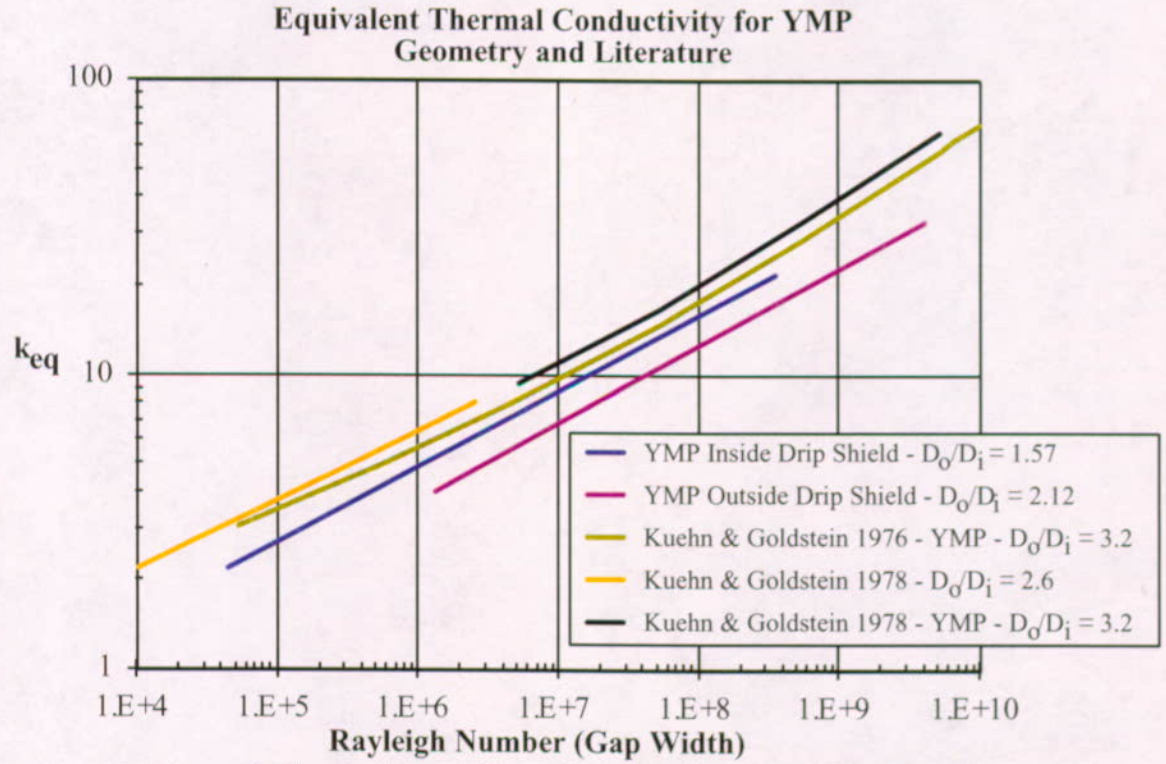

Figure 2. Comparison of Natural Convection Correlation Equations

As shown in Figure 2, CFD-based equivalent thermal conductivity values are lower than those of Kuehn and Goldstein (1976b, 1978). This indicates that geometry affects the average equivalent thermal conductivity associated with the YMP annulus. The heat transfer correlation equations developed in the literature are specifically for the annulus formed by horizontal concentric cylinders. In some instances allowances are made for eccentric placement of the inner cylinder in the correlation equations in the literature. However, these expressions do not account for changes in heat transfer due to flow blockages (e.g., invert, drip shield). It is clear that the YMP geometry with invert and drip shield is not adequately represented by literature correlation equations developed for an annulus formed by horizontal concentric cylinders.

2.2 Equivalent Thermal Conductivity Obtained Using Kuehn and Goldstein (1978) Correlations

For comparison purposes the equivalent thermal conductivity was also obtained using the correlations of Kuehn and Goldstein (1978). In developing equivalent thermal conductivity correlations for this case, separate calculations were made for the volume inside and outside of the drip shield. Because the Kuehn and Goldstein method is based on concentric cylinders, approximations were made in the YMP geometry to obtain inner and outer radii of the cylinders. In this study, the inner cylinder was represented by a single waste package diameter representing an average waste package diameter (radius = 0.856 m). For the outer cylinder an effective radius was calculated representing the drip shield and the inner invert. This value was obtained using the characteristic gap width previously calculated (0.485 m) and the waste package radius (0.856 m). The gap width for two concentric cylinders is equal to the difference between the outer and inner radii. Because the inner radius (waste package) and the gap width are known, the approximate outer radius was calculated to be 1.341 m. Outside the drip shield the inner cylinder radius is the outer radius of inside the drip shield. An approximate outer radius was obtained using the previously calculated gap width (1.5 m) and the inner radius (1.341 m) to be 2.841 m.

Using these approximate inner and outer cylinder radii and the Kuehn and Goldstein correlations, calculations were done to evaluate equivalent thermal conductivities for the regions inside and outside the drip shield. The correlation equations are shown in Table 2.

Table 2. Summary of YMP Correlation Equations for Natural Convection Heat Transfer in Enclosures based on Kuehn and Goldstein (1978) Calculations[1]

Location	Correlation Equation	Comments	Eq.
Inside Drip Shield	$k_{eq} = 0.052 Ra_{Lc}^{0.282}$	$1.88x10^6 \le Ra_{L_c} \le 1.88x10^9$	9
	$k_{eq} = 18{,}584 \overline{T}^{1.329} \Delta T^{0.282} L_c^{0.847}$	0.002 K $\le \Delta T \le$ 20 °C, L_c = 0.485m, $\overline{T}$ is the average fluid temperature in K	10
Outside Drip Shield	$k_{eq} = 0.057 Ra_{Lc}^{0.296}$	$1.79x10^7 \le Ra_{L_c} \le 1.79x10^{10}$	11
	$k_{eq} = 36{,}285 \overline{T}^{1.391} \Delta T^{0.296} L_c^{0.88}$	0.002 K $\le \Delta T \le$ 20 °C, L_c =1.5m, $\overline{T}$ is the average fluid temperature in K	12

1 - $k_{eff} = k_{eq} * k_a(\overline{T})$

3. MODEL DESCRIPTION

This section describes modeling that was done to compare CFD natural convection results with those of conduction-only models that used the equivalent thermal conductivity. The FLUENT CFD code was used for all simulations with heat generation boundary condition at the waste package and a constant temperature boundary condition 5 meters into the host rock. The assumption is made that a quasi-steady-state condition exists which implies that the rate of temperature changes five meters into the rock is small enough that the volume inside of this region can be considered as a steady-state model. A description of the model is given below.

3.1 Model Geometry

As described in the introduction the geometry used in this study consists of an emplacement drift, a waste package, a drip shield, and an invert (Figure 1). The geometry thus consists of two enclosed annuli: the inner annulus bounded by the waste package, the drip shield and the inside of the invert, and the outer annulus bounded by the drip shield, drift wall and outer invert. The invert provides a flow blockage at the bottom. The configuration represents a heated inner cylinder and a cooler outer cylinder.

The geometric parameters of the model are shown in Table 3 and illustrated in Figure 3. The waste package is represented by the average waste package diameter. The geometries of the other drift components are as given in Francis et al. (2003). The domain for the drift CFD models is a half-cylinder 15.5 m in diameter including the rock. A shell of host rock five meters thick is

on the outer surface of the cylinder. To reduce computational costs, only half of the drift was modeled. A symmetry plane was located at the center of the drift. Figure 3 shows the computational grid used in the CFD simulations.

Table 3: Geometry of YMP model components

Waste Pakage Diameter	Drift Diameter	Invert Height	Outside Width of drip shield	Height of drip shield	Outer rock diameter
1.711 m	5.5 m	0.81 m	2.51 m	2.521 m	15.5 m

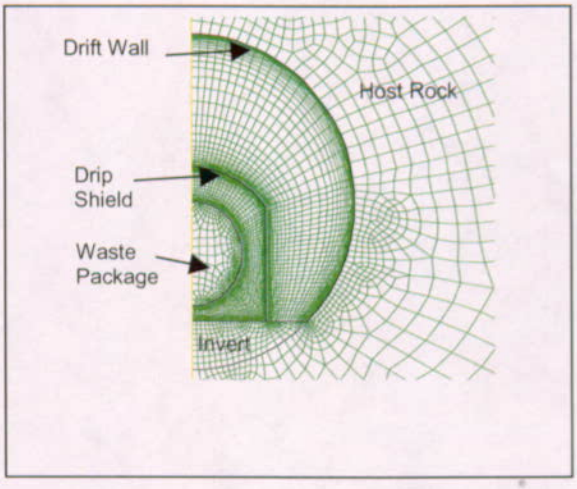

Figure 3. Illustration of the Geometry and Mesh used in the Two-Dimensional FLUENT Models

3.2 Material and Fluid Properties

Thermal properties of the engineered barrier system components are given in Table 4 below. These properties are relevant to steady state modeling.

Table 4: Material properties of model components

Material	Thermal Conductivity [W/m K]	Emissivity
Waste Package	1.5	0.87
Drip Shield	20.708	0.63
Invert (Crushed Tuff)	0.2	0.9
Repository Host Rock	1.8895	0.9

Properties of air were taken from Incropera and Dewitt (1990).

3.3 Boundary Conditions

For the waste package, invert, and the host rock, a no heat flux boundary condition was imposed on the center-line symmetry faces (Figure 3). For the inner and outer drip shield air volumes, a no heat flux, no mass flux, and a velocity slip condition was imposed on the center-line symmetry face. For all of the solid-air interfaces, a no mass flux, no-slip boundary condition is imposed. The FLUENT code balances heat flux at those solid-air interfaces within the model. The heat is introduced into the model through a volumetric heat generation rate inside the waste package. Heat is removed from the model as a result of the constant temperature boundary condition imposed on the outer boundary of the host rock.

3.3.1 Heat Load

The decaying heat of the waste packages is dependent on the waste package type and length. For this study the heat load of a waste package containing 21 pressurized water reactor fuel assemblies (21-PWR, hot) has been used. Table 5 shows the values of nominal time-dependent decay heat for the waste package.

Table 5 Design basis repository power output for 21-PWR (Hot) waste package

Time [Years]	21-PWR AP (Hot) [W/m^3]
300	118.75
1000	50.45
3000	20.80

3.3.2 Boundary Rock Temperature

Boundary rock temperatures (5m into the rock) are given in Table 6 for the specified time periods. Rock temperatures were approximated using conduction line source solutions and superposition at a typical location within the repository. This assumption assumes a quasi-steady state solution in the model domain.

Table 6 Rock boundary temperatures (5m from drift wall)

Time [Years]	Temperature [°C]
300	96.15
1000	87.15
3000	66.15

3.4 Operating Conditions

A quasi-steady state was assumed in all FLUENT simulations at the selected repository periods (300, 1000 and 3000 Years). The operating pressure selected for the numerical simulations is

89.05 kPa, which is the standard atmospheric pressure at the elevation of the repository. Standard atmospheric pressure at sea level is selected to perform a comparison to literature heat transfer results for natural convection (both data and correlation equations). The specified initial gauge pressure is 0 Pa for each simulation. The absolute pressure is computed by the CFD code as the operating pressure plus the gage pressure, or 89.05 kPa in this case. Gravity is specified in each of the simulations in this study as 9.81 m/s^2.

3.5 Summary of the Computational Model

The CFD numerical simulation settings and runtime monitoring for equation residuals, discretization, convergence, and steady-state energy balance are described in this section for all the models.

The steady-state segregated solver in FLUENT is used in this work. The segregated solver approach results in the governing equations being solved sequentially. An implicit linearization technique is applied in the segregated solution of the modeled equations previously described. This results in a linear system of equations at each computational cell. The equations are coupled and non-linear; therefore, several iterations of the equation set are required to obtain a converged solution. A Renormalization Group (RNG) k-ε turbulent flow model using enhanced wall treatment was selected for use because it gives superior predictions for rapidly straining flows as well as better estimates of wall heat transfer than the standard k-ε model. The mesh was refined to give y+ values (a dimensionless distance from the wall based on fluid properties and flow conditions) less than or equal to one. The discrete ordinates model (DO) with angular discretizations all set to six was used to model thermal radiation. In all the simulations in this work, the air inside the enclosures was treated as a radiative non participating fluid. Details of the computational approach are given by Webb and Itamura. (2004).

FLUENT uses a control-volume method to solve the governing equations. The equations are discrete for each computational cell. In applying this solution method the CFD simulation stores flow properties (e.g., dependent variables) at cell centers. However, face values are required for the convection terms in the discretized equations. Face values are obtained by interpolation from the cell centers using a second-order upwind scheme for the momentum and energy equations and a first-order upwind scheme for the turbulence equations. It is noted that the diffusion terms in the equations are central-differenced and are second-order accurate. The body-force-weighted pressure interpolation scheme is applied to this analysis. The pressure interpolation scheme is used to compute face pressures from cell center values. A body-force-weighted pressure interpolation scheme is applicable to buoyancy driven flows. Pressure-velocity coupling is achieved through the SIMPLE (Semi-Implicit Method for Pressure-Linked Equations) algorithm. The SIMPLE algorithm uses the discrete continuity equation to determine a cell pressure correction equation. Once a solution to the cell pressure correction equation is obtained the cell pressure and face mass fluxes are then corrected using the cell pressure correction term.

The flow solution is given an arbitrary initial starting point for fluid velocity, temperature, and turbulence quantities. Additional iterations are required for solution convergence. A flow solution is considered to have converged after all equation residuals have been reduced by several orders of magnitude. A final convergence criteria specified in the CFD simulations is

based on an overall steady-state energy balance. In addition changes in variables such as temperature and velocity are monitored for convergence. When the energy imbalance is about 0.5% or less and changes in variables are low, it is assumed that stead-state is reached and the flow simulation is complete.

4. COMPUTATION RESULTS

FLUENT calculations were carried out with a 21 PWR (hot) heat generation source at three different time periods after repository waste emplacement: 300 years, 1000 years and 3000 years. For each case considered two calculations were done: natural convection (termed CFD), and conduction only with equivalent thermal conductivities obtained using a User Defined Function (A FLUENT macro containing the equivalent thermal conductivity correlations) (termed ETC). To compare results of CFD based equivalent thermal conductivities (i.e. ETC) with those of Kuehn and Goldstein (1978) correlations, additional FLUENT calculations were also made with the 21 PWR (hot) power source at the three time periods. The Kuehn and Goldstein based conduction calculations (termed K&G) are discussed in Section 4.2.

4.1 Comparison of CFD and Conduction only ETC results

Three calculations were performed at the selected three time periods.

4.1.1 Average Temperatures

At 300 years, the heat generation rates of waste packages are still relatively high. Table 7 shows average temperature predictions for the different surfaces and the air inside and outside the drip shield for the three types of FLUENT calculations at 300 years. The waste package temperatures for this case are high due to the high heat source and high rock temperature boundary condition. The CFD predicted average waste package temperature is 132.04 °C, which is above boiling. Since these calculations are for single-phase airflow, evaporation of water (phase change) is not modeled. As shown in Table 7 the ETC over predicted the CFD average waste package temperature by about 0.35 °C. Predictions of average drip shield and drift wall temperatures ETC were about the same as those of the CFD. ETC predictions of inner invert and outer invert average temperatures were higher than those of the CFD by about 1.02 °C and 0.48 °C respectively. The predicted average air temperature inside the drip shield for ETC is higher than the CFD by about 0.2 °C. The predicted average air temperature outside the drip shield for ETC is lower than the CFD by about 0.26 °C.

Table 7: Calculated Average temperature [°C] at 300 years

Body	CFD	ETC	CFD-ETC
Waste Package	132.04	132.38	-0.34
Drip Shield	126.31	126.35	-0.04
Drift Wall	122.20	122.11	0.08
Inner-Invert	130.02	131.04	-1.02
Outer-Invert	122.82	123.3	-0.48
Inner-Air	129.1	129.3	-0.2
Outer-Air	123.85	123.59	0.26

At 1000 years decaying of the heat source has significantly reduced the heat generation rates of waste packages. Table 8 shows average temperature predictions for the different surfaces and the air inside and outside the drip shield for the three types of FLUENT calculations at 1000 years. The waste package temperatures for this case are still high due to the significant heat source and high rock temperature boundary condition. The CFD predicted average waste package temperature is 103.85 °C, which is slightly above boiling for the location. As shown in Table 8 the ETC over predicted the CFD average waste package temperature by about 0.18 K, which is about half of the 300-year case. Predictions of average drip shield and drift wall temperatures of ETC were about the same as those of the CFD. ETC predictions of inner invert and outer invert average temperatures were higher than those of the CFD by about 0.54 °C and 0.25 °C respectively. The predicted average air temperature inside the drip shield for ETC is higher than the CFD by about 0.1 °C. The predicted average air temperature outside the drip shield for ETC is lower than the CFD by about 0.13 °C. Overall, the heat generation rate at 1000 years is less than half of that at 300 years, and temperature predictions for the conduction only calculations and CFD are reduced by about half.

Table 8: Calculated Average temperature [°C] at 1000 years

Body	CFD	ETC	CFD-ETC
Waste Package	103.849	104.03	-0.181
Drip Shield	100.893	100.916	-0.023
Drift Wall	98.797	98.753	0.044
Inner-Invert	102.731	103.274	-0.543
Outer-Invert	99.116	99.364	-0.248
Inner-Air	102.342	102.434	-0.092
Outer-Air	99.643	99.509	0.134

At 3000 years decaying of the heat source has significantly reduced the heat generation rates of waste packages. Table 9 shows average temperature predictions for the different surfaces and the air inside and outside the drip shield for the three types of FLUENT calculations at 3000 years. The waste package temperatures for this case are much lower than those of the 300-year and 1000-year calculations due to the much lower heat source and relatively lower rock temperature

boundary condition. The CFD predicted average waste package temperature is 73.30 °C, which is below boiling. As shown in Table 9 the ETC over predicted the CFD average waste package temperature by about 0.1 °C. Predictions of average drip shield and drift wall temperatures of ETC were about the same as those of the CFD. ETC predictions of inner invert and outer invert average temperatures were higher than those of the CFD by about 0.29 °C and 0.13 °C respectively. The predicted average air temperature inside the drip shield for ETC is higher than the CFD by about 0.05 °C. The predicted average air temperature outside the drip shield for ETC is lower than the CFD by about 0.07 °C.

Table 9: Calculated Average temperature [°C] at 3000 years

Body	CFD	ETC	CFD-ETC
Waste Package	73.302	73.401	-0.099
Drip Shield	71.775	71.788	-0.013
Drift Wall	70.694	70.67	0.024
Inner-Invert	72.678	72.968	-0.29
Outer-Invert	70.859	70.994	-0.135
Inner-Air	72.517	72.572	-0.055
Outer-Air	71.132	71.062	0.07

Comparing the CFD results in Tables 7 to 9 periods the average air temperature inside the drip shield is lower than the average inner invert surface temperature. This indicates that heat is transferred from the inner invert to the air. The hot surface on the inner invert is caused by thermal radiation from the waste package. For the region outside the drip shield the average air temperature is higher than the average drift wall temperature and outer invert. Thus, heat is transferred from the air to these surfaces. At the local pressure (89.05 kPa) the boiling point is about 96 °C. Thus, the average temperatures at all surfaces for the 300-year calculations are above boiling. For the 1000-year calculations temperatures are near the boiling temperature and for the 3000-year calculations temperatures are below boiling. The differences in temperature indicate that there is a potential for moisture movement inside the drift. Note that local variations exist as shown in the temperature profile plots. Table 10 shows equivalent thermal conductivity and Rayleigh number values at the three times. The Rayleigh numbers indicate that the flow is turbulent in all cases.

Table 10: Equivalent thermal conductivity and Gap-width Rayleigh number for the CFD calculations at the three times.

Time [Year]	Ra_{L_c} Inside Drip Shield	k_{eq} Inside Drip Shield	Ra_{L_c} Outside Drip Shield	k_{eq} Outside Drip Shield
300	1.28×10^7	9.68	3.22×10^8	17.29
1000	9.21×10^6	8.89	2.20×10^8	15.65
3000	7.09×10^6	8.31	1.65×10^8	14.50

4.1.2 Surface Temperature Profiles

Figure 4 illustrates the local temperature variations predicted of CFD and ETC simulations at the 300-year time period for all surfaces. Figure 5 shows waste package surface temperatures versus vertical position for 300 years. As shown in Figures 5 some prediction differences exist between CFD and ETC all along the length of the surface. ETC under predicts local temperatures on the upper part of the waste package surface but over predicts for the rest of the surface. For the 300-year calculations the largest differences are at the bottom of the waste package where the ETC model over predicts temperatures by as much as 1.70 °C. For the 1000-year and 3000-year calculations the corresponding over predictions are 0.87 °C and 0.42 °C, respectively.

Similar temperature profiles of the waste package surface were obtained for 1000 and 3000 years, with lower temperatures. This shows that the waste package surface temperatures vary with position and time period. Due to the higher power generation the variation with position is larger at the earliest time (i.e. 300 years). [Also, Tables 7 to 9 and the temperature profiles show that both the average and local temperatures are highest at the earlier time. This is true for all surfaces.]

As with the average temperature predictions (Tables 7 to 9) temperature profiles for the drip shield and drift wall surfaces of CFD and ETC at all time periods are very close to each other (see Figure 4 for 300-year results). ETC local temperature predictions on these surfaces are similar to those of the CFD. Figure 6 shows temperature profiles for combined inner and outer invert surfaces for 300 years. The inner invert extends from 0 to 1.25 m and the outer invert from 1.25 m to 1.95 m. The results at the three time periods show that for the inner invert ETC local temperatures over predict those of the CFD by as much as about 1.5 °C for 300-year calculations (Figure 6), 0.80 for 1000-year calculations and 0.4 for 3000-year calculations. The largest differences are at locations near the waste package. Away from the waste package the differences in the predicted local temperatures are reduced and about zero at the drip shield . In the outer invert the differences at both ends (drip shield and drift wall) are minimal. Some differences exist at locations between the ends.

Plots of temperature versus position for specified lines measured from the center of the waste package are shown in Figure 7 for the 300-year time period. The positive vertical symmetry line is at zero degrees. The width of the two annular spaces varies depending on the inclination of the line. The lines show gradual temperature reduction from the waste package to the outer edge of the rock formation. For the CFD case the flatter parts of the lines represent the temperatures in the air inside and outside the drip shield, showing gradual temperature variations in the open spaces within an line. However, the different lines show that air temperatures are higher near the top, a result of an upward moving air by natural convection. The sharp drops at the beginning or end of the flat CFD lines (i.e. near surfaces) indicate boundary layer behavior. For the ETC, temperature changes across the open spaces are more pronounced, indicative of temperature gradient by conduction across a body. The ETC predicts higher air temperatures at the bottom. As expected both the CFD and ETC simulations give the same result for conduction through solid materials.

For the CFD simulations, heat transfer by thermal radiation and natural convection influence the temperature predictions. For the ETC simulations, thermal radiation and conduction are important. However, the effect of thermal radiation on temperature is more important than both natural convection and conduction. Figure 8 shows convective (CFD) and conductive (ETC) flux variations at the waste package surface for the 300-year time period. The plots show that for the most part the convective flux (CFD) increases from top to bottom. The conductive flux (ETC) does not follow the same pattern. For the ETC the conductive flux variations reflect distances between surfaces of the inner annular space. Thus, the heat flux increases as the distance between surfaces is reduced.

It is clear from the results shown that the conduction only temperature profiles do not always replicate the CFD local temperature variations. The differences in temperature profiles reflect the use of a constant equivalent thermal conductivity for each open space. As shown in Francis et al. (2003) the equivalent thermal conductivity varies with location. But in many locations the differences in predicted temperatures are minimal, and thus the conduction only simulations reasonably replicate CFD results. Also, if the average temperature is sufficient, as in many applications at YMP, then the conduction only simulation results could be a good substitute for turbulent natural convection. Evaporation and condensation can occur inside of the drift. As shown in Tables 7 to 9 and the temperature profile plots the CFD and ETC temperature predictions at the cooler surfaces are very close. Prediction discrepancies are more pronounced at hotter surfaces. Thus, it can be concluded that use of the conduction only results would have minimal adverse effects for the possible occurrence of condensation. As stated in Section 1 the equivalent thermal conductivity method was not designed for multiphase flows, and the two-dimensional modeling approach may potentially mask axial variations in temperature. [The use of the equivalent thermal conductivity correlations assumes that flow patterns are known, which in this case represent 2-D. Differences in 2-D versus 3-D simulation are discussed by Itamura et al. (2004). Future work, comparing 3-D drift temperatures from CFD calculations with 2-D equivalent thermal conductivity predictions, is underway.]

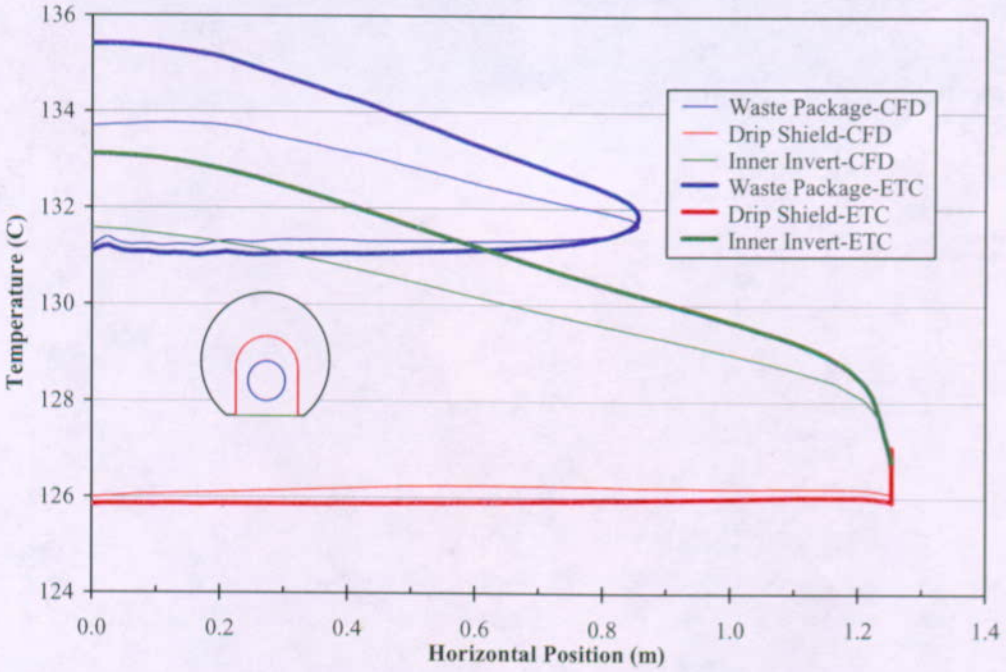

Fig. 4a Surface Temperature Predictions at 300 Years: CFD and ETC (Inside Drip Shield)

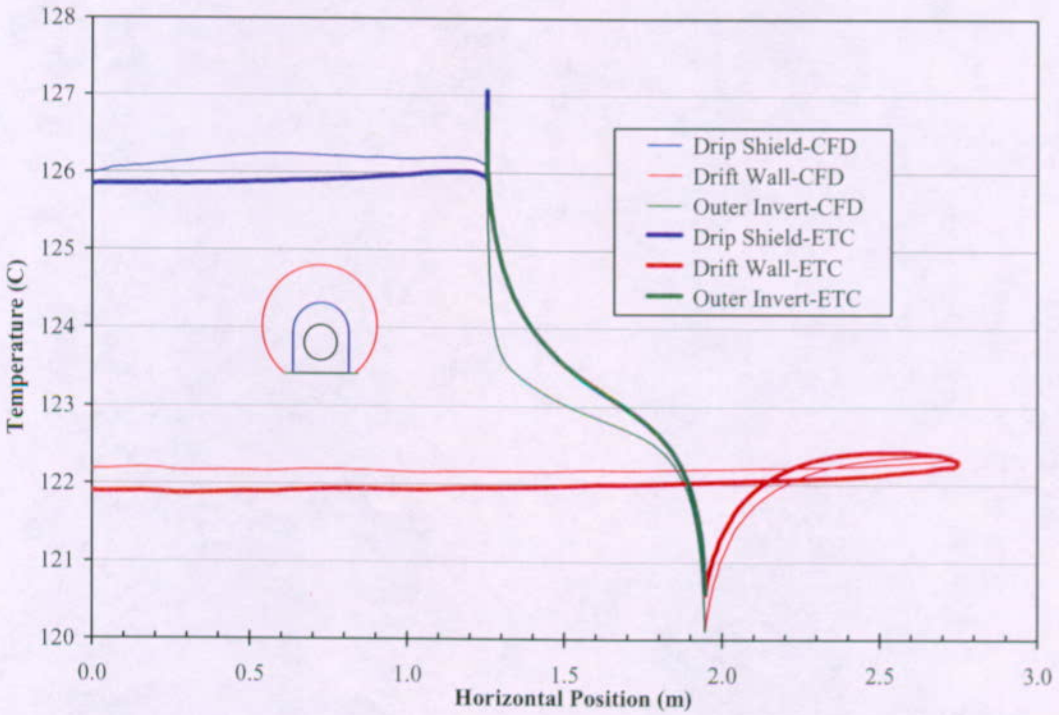

Fig. 4b Surface Temperature Predictions at 300 Years: CFD and ETC (Outside Drip Shield)

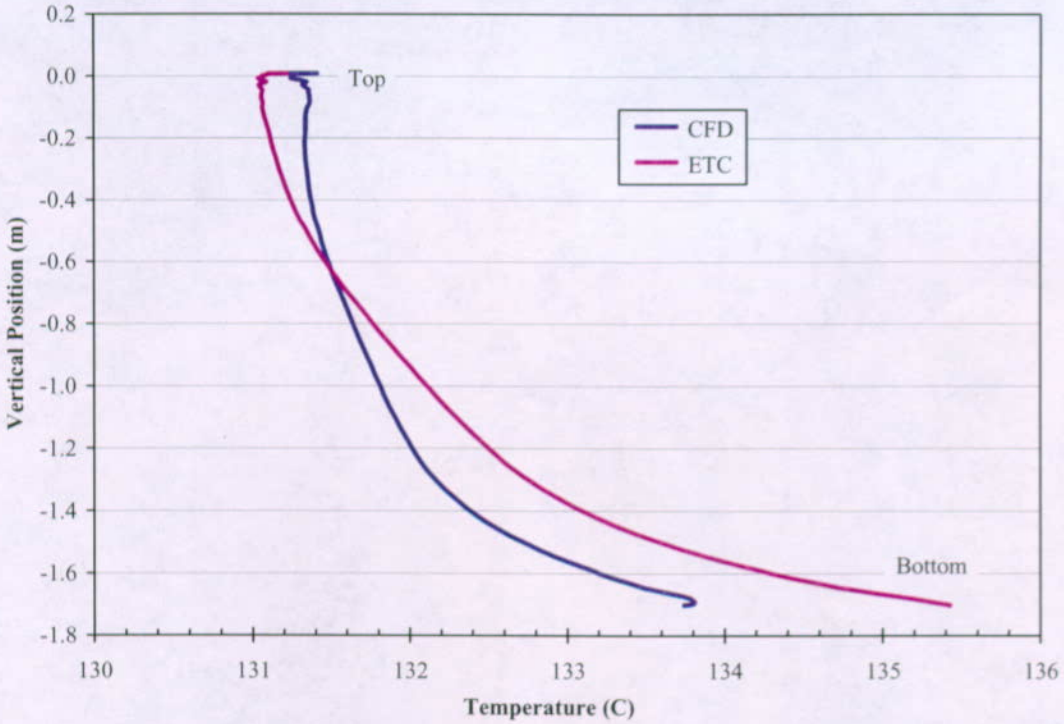

Fig. 5 Waste Package Surface Temperature at 300 Years

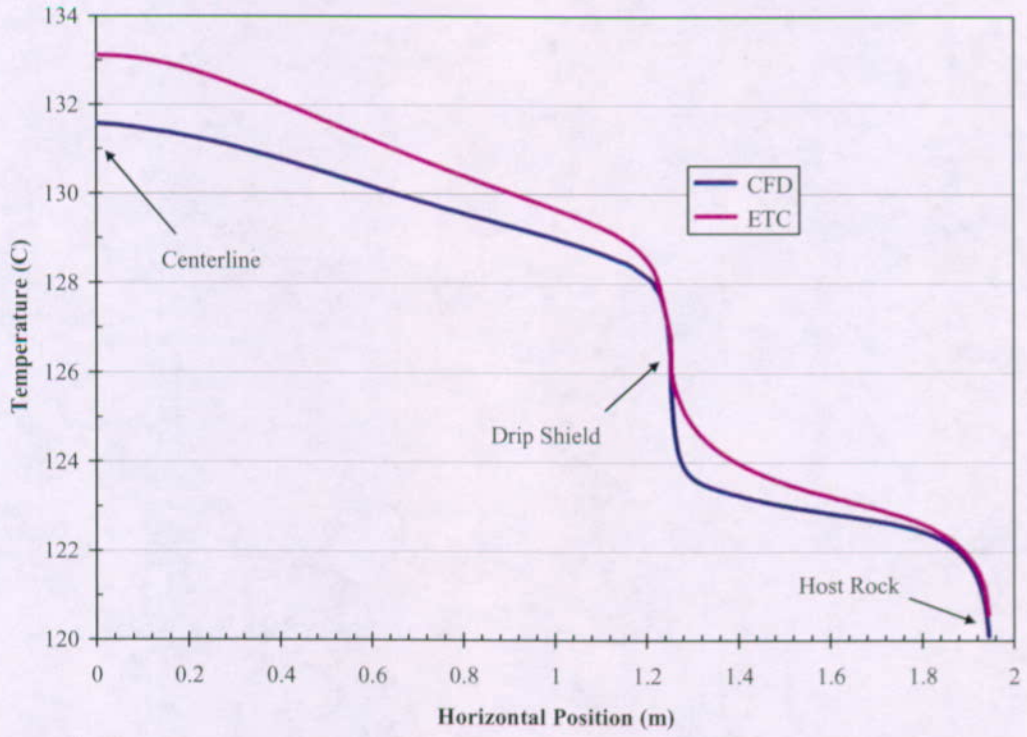

Fig. 6 Invert Surface Temperature at 300 Years

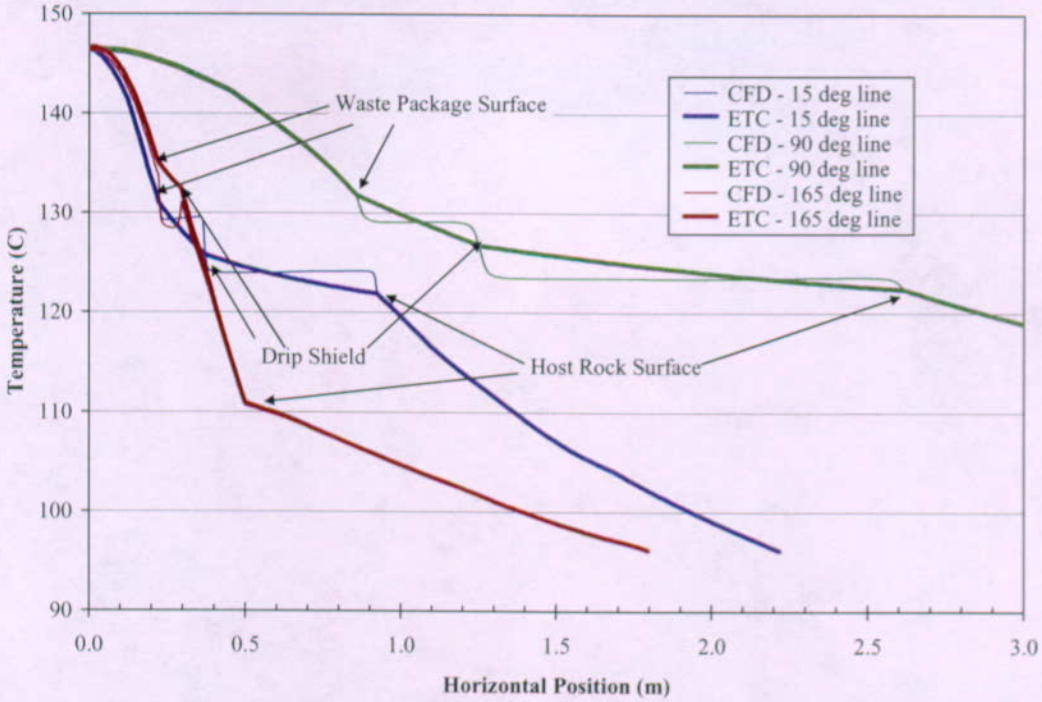

Fig. 7 Temperature Predictions Along 15°, 90°, and 165° Lines (from top of waste package) at 300 Years

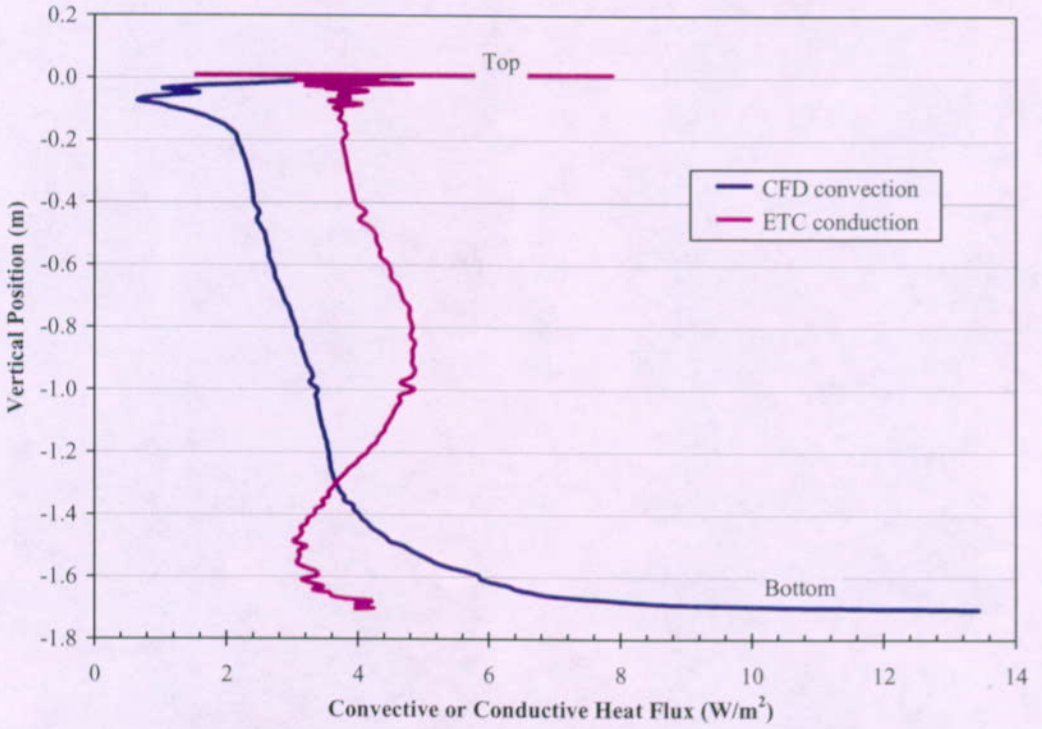

Fig. 8 Waste Package Surface Convective (CFD) and Conductive (ETC) Heat Flux at 300 Years

4.2 Comparison of CFD and Kuehn and Goldstein (1978) based Conduction-only Model Results

Results of the Kuehn and Goldstein based FLUENT simulations are given in Table 11 and Figures 9 and 10 together with the CFD and ETC predictions. Table 11 shows that average temperature predictions of Kuehn and Goldstein based conduction-only calculations (K&G) are similar to those of CFD-based calculations (ETC). However, variations exist in local temperature predictions (see Figures 9 and 10). In Figure 10 the K&G temperature curve is to the left of the ETC curve. At the bottom of the waste package the K&G temperatures are slightly closer to those of the CFD than those of the ETC. The K&G temperature predictions are worse at the top of the waste package. The results show that although the equivalent thermal conductivity correlations for both the ETC and K&G were based on approximately similar geometry, the underlying Kuehn and Goldstein (1978) method was not designed for the complex YMP geometry.

Table 11: Calculated Average temperature [°C] at 300 years

Body	CFD	ETC	K&G	CFD-ETC	CFD-K&G
Waste Package	132.036	132.383	132.52	-0.347	-0.484
Drip Shield	126.306	126.351	126.288	-0.045	0.018
Drift Wall	122.195	122.109	122.105	0.086	0.090
Inner-Invert	130.017	131.042	131.101	-1.025	-1.084
Outer-Invert	122.819	123.297	123.324	-0.478	-0.505
Inner-Air	129.097	129.304	129.332	-0.207	-0.235
Outer-Air	123.846	123.589	123.438	0.257	0.408

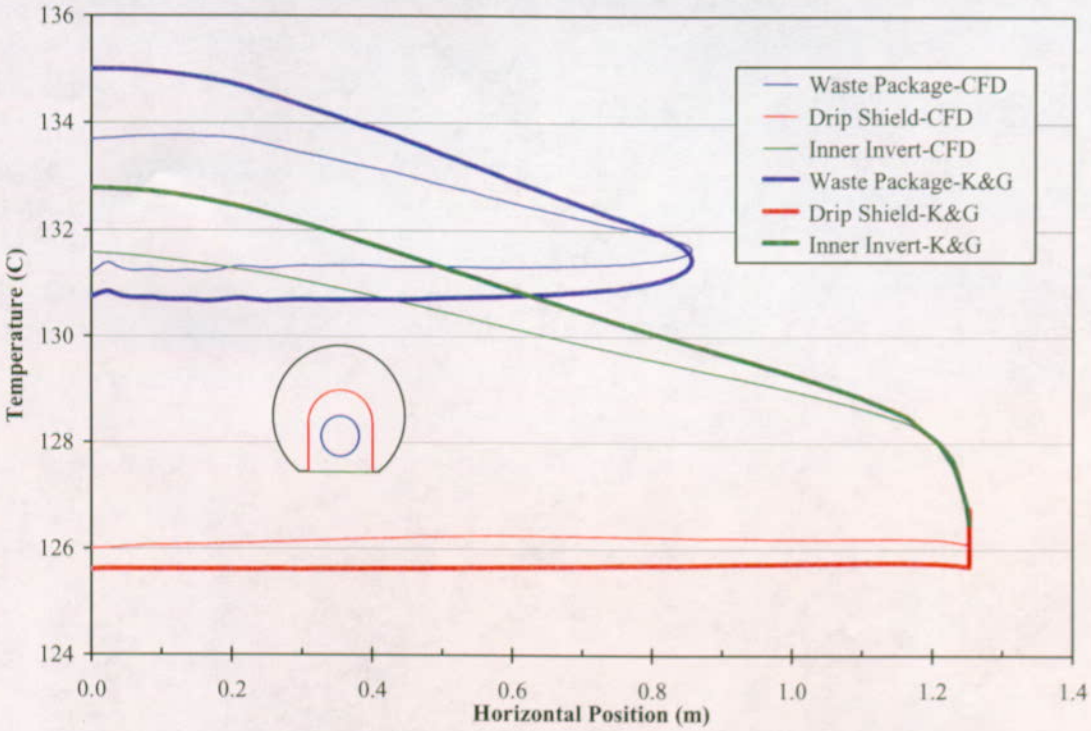

Fig. 9a Surface Temperature Predictions at 300 Years: CFD and K&G (Inside Drip Shield)

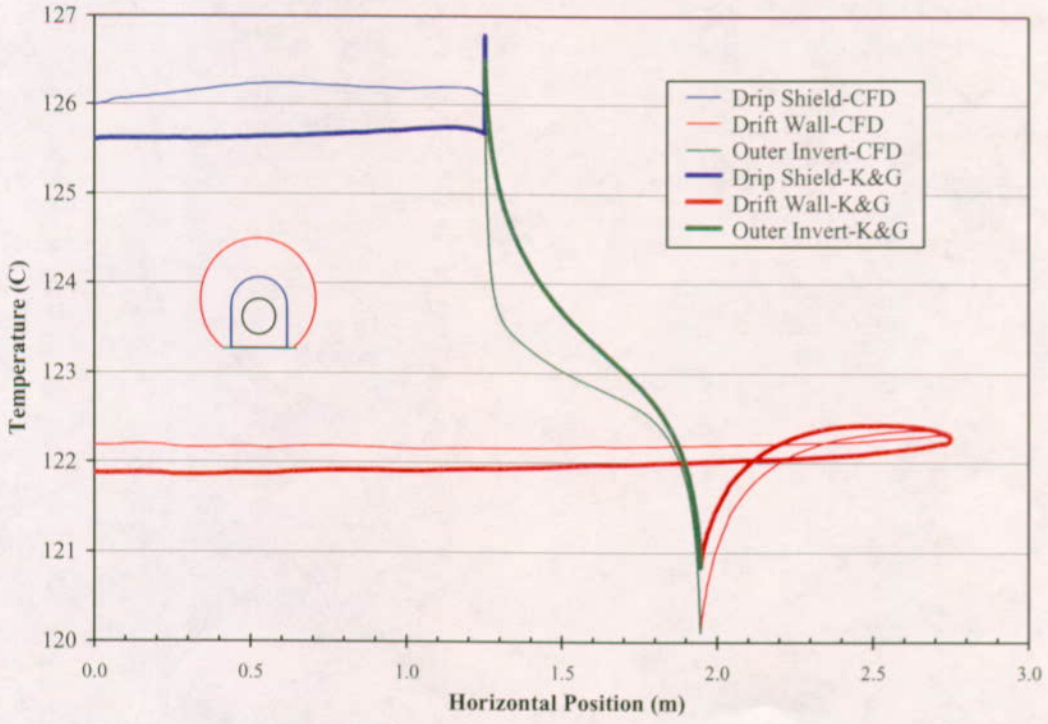

Fig. 9b Surface Temperature Predictions at 300 Years: CFD and K&G (Outside Drip Shield)

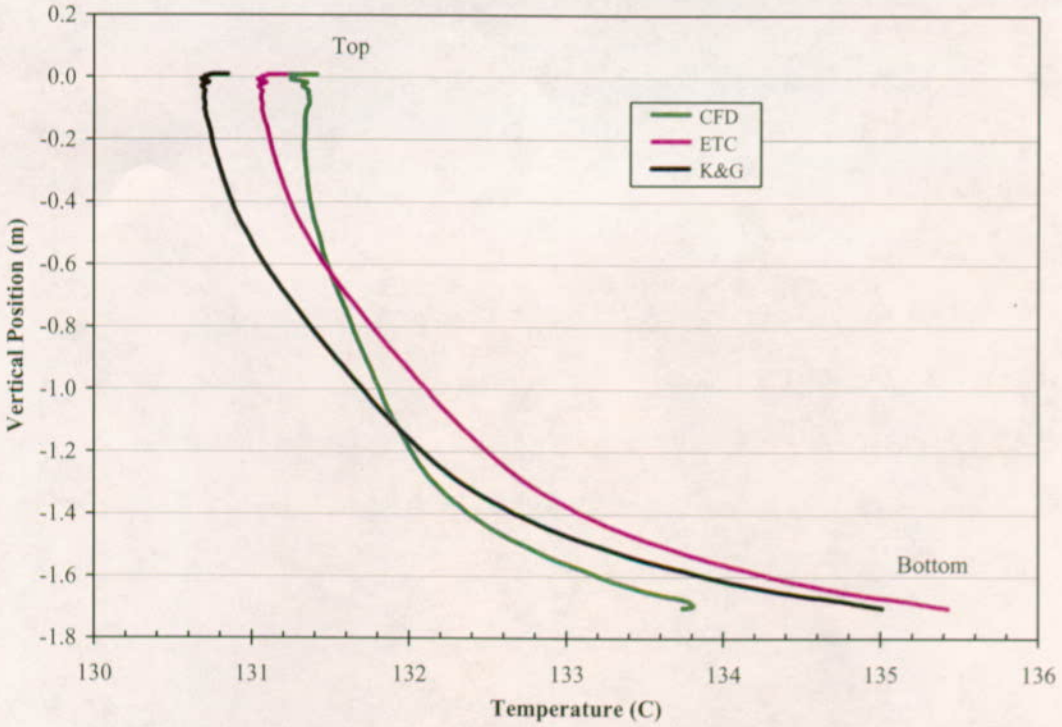

Fig. 10: Comparison of Waste Package Surface Temperature Predictions 300 Years: CFD, ETC, K&G

5. CONCLUSIONS

A two-dimensional heat transfer model representing the YMP geometry was used to compare CFD temperature simulation results against conduction-only simulations that use equivalent thermal conductivity correlations. The FLUENT code was used for all simulations with heat generation boundary condition at the waste package and constant temperature boundary condition 5 meters into the rock formation. For the simulations three repository time periods, with corresponding heat generation and rock temperature boundary conditions were selected. All simulations included thermal radiation between surfaces.

The results show for the two-dimensional YMP geometry and simulation conditions considered, the average surface temperatures of the CFD natural convection and conduction-only using the equivalent thermal conductivity are similar while maximum local temperature differences for the different surfaces were within two degrees. The differences in temperature profiles reflect the use of a constant equivalent thermal conductivity. If the average temperature is what is required, as in many applications at YMP, then the conduction only simulation results could be a good substitute for the more expensive turbulent natural convection models.

Condensation could occur at cooler surfaces if the local vapor pressure of water is high enough. However, the local temperature predictions of the CFD and ETC cases at the cooler surfaces are very close. This would indicate that use of the conduction only results would have minimal adverse effects for the ability to predict condensation. The equivalent thermal conductivity

method was not designed for multiphase flows, and the two-dimensional modeling approach may potentially mask variations in temperature down the drift.

The Kuehn and Goldstein (1978) method was also used to provide equivalent thermal conductivity correlations for comparison with the CFD-based correlations. Results showed that although the equivalent thermal conductivity correlations for both methods were based on approximately similar geometry, the Kuehn and Goldstein (1978) method over predicts the turbulent natural convection, which results in lower temperatures.

The use of the equivalent thermal conductivity correlations assumes that flow patterns are known, which in this case represent 2-D. Differences in 2-D versus 3-D simulation are discussed by Itamura et al. (2004). Work comparing 3-D drift temperatures from CFD calculations with 2-D equivalent thermal conductivity predictions is currently underway.

6. ACKNOWLEDGEMENTS

The authors would like to thank Darryl James of Texas Tech University in Lubbock, Texas for his contribution in providing a user defined function for effective thermal conductivity calculation. This work was supported by the Yucca Mountain Site Characterization Office as part of the Office of Civilian Radioactive Waste Management (OCRWM), which is managed by the U.S. Department of Energy, Yucca Mountain Site Characterization Project. Sandia is a multiprogram laboratory operated by Sandia Corporation, a Lockheed Martin Company, for the United States Department of Energy under Contract DE-AC04-94AL85000.

7. REFERENCES

Fluent Incorporated 2001. *FLUENT 6 User's Guide.* Volumes 1 to 5. Lebanon, New Hampshire: FLUENT Incorporated.

Francis, N.D., Jr.; Itamura, M.T.; Webb, S.W.; and James, D.L. 2002. *CFD Calculation of Internal Natural Convection in the Annulus Between Horizontal Concentric Cylinders.* SAND2002-3132. Albuquerque, New Mexico: Sandia National Laboratories.

Francis, N.D.,Jr.; Webb, S.W.; Itamura, M.T.; and James, D.L. 2003. *CFD Modeling of Natural Convection Heat Transfer and Fluid Flow in Yucca Mountain Project (YMP) Enclosures.* SAND2002-4179. Albuquerque, New Mexico: Sandia National Laboratories.

Incropera, F.P. and DeWitt, D.P. 1990. *Fundamentals of Heat and Mass Transfer.* 3rd Edition. New York, New York: John Wiley & Sons.

Itamura, M.T.; Francis, N.D.,Jr.; and Webb, S.W. 2004. In-Drift Natural Convection Analysis of the Low Temperature Operating Mode Design. Submitted for publication in *Nuclear Technology.*

Kuehn, T.H. and Goldstein, R.J. 1976. "Correlating Equations for Natural Convection Heat Transfer Between Horizontal Circular Cylinders." *International Journal of Heat and Mass Transfer, 19,* (10), 1127-1134. New York, New York: Pergamon Press.

Kuehn, T.H. and Goldstein, R.J. 1978. "An Experimental Study of Natural Convection Heat Transfer in Concentric and Eccentric Horizontal Cylindrical Annuli." *Journal of Heat Transfer, 100,* ([4]), 635-640. [New York, New York: American Society of Mechanical Engineers].

Webb, S.W., Francis, N.D., Dunn, S.D., Itamura, M.T., and James, D.L. 2003. "Thermally-Induced Natural Convection Effects in Yucca Mountain Drifts." *Journal of Contaminant Hydrology.* Volume 62-63, pp. 713-730.

Webb, S.W., and M.T. Itamura, 2004, "Calculation of Post-Closure Natural Convection Heat and Mass Transfer in Yucca mountain Drifts," ASME Paper HT-FED2004-56611, these proceedings.